Square well/barrier resonances in the potentiodynamic plane

Meeten, Ryan P; Morozov, Gregory V

Published in:
Physics Letters A

Published: 28/09/2020

Square Well/Barrier Resonances in the Potentiodynamic Plane

R. P. Meeten and G. V. Morozov*

Scottish Universities Physics Alliance (SUPA), Institute of Thin Films, Sensors and Imaging, University of the West of Scotland

(Dated: July 3, 2020)

The complex wave number plane equips us with an elegant mathematical construct which can be used to display and classify the different types of states which arise from solution of the time-independent Schrödinger equation for a quantum mechanical potential. The complex wave number plane is also useful for tracking the trajectories of these solutions as the potential is perturbed in some way, often resulting in profound dynamical structure. In this work we propose an alternative coordinate system, which we call the *potentiodynamic plane*, which has the useful property that the trajectories stay bounded, and apply this to the square well potential to reveal some new insights.

I. INTRODUCTION

Resonances and resonant phenomena appear in many branches of mathematics, physics, and engineering. They are especially important in the fields of semiconductor nanostructures, microcavity lasers, and biosensing, see Refs. [1–4].

In quantum mechanics the concept of a resonant state (resonance) is a natural extension of the idea of a bound state. It was introduced in Refs. [5, 6] and it is sometimes referred as the Gamow vector. The coordinate parts of resonant states $\psi_n(\mathbf{r})$ are solutions of the time-independent Schrödinger equation,

$$[-\Delta + V(\mathbf{r})]\, \psi(\mathbf{r}) = \mathcal{E}\psi(\mathbf{r}) \tag{1}$$

with complex eigenvalues

$$\mathcal{E}_n = E_n - \frac{1}{2} i\Gamma_n, \quad \Gamma_n > 0\,, \tag{2}$$

on which the outgoing boundary conditions are imposed, see Eqs. (5, 6) for details. The overall wave functions $\Psi_n(\mathbf{r}, t)$ of resonant states decay in time in accordance with

$$\Psi_n(\mathbf{r}, t) = \psi_n(\mathbf{r}) \exp(-iE_n t) \exp(-\Gamma_n/2t)\,. \tag{3}$$

In obeyance with time-reversal invariance, the above resonant states should be accompanied by another set of solutions of Eq. (1), which have the form $\psi_{-n}(\mathbf{r}) = \psi^*_n(\mathbf{r})$, with the corresponding eigenvalues $\mathcal{E}_{-n} = \mathcal{E}^*_n$, and the overall wave functions $\Psi_{-n}(\mathbf{r}, t) = \Psi^*_n(\mathbf{r}, -t)$, *i.e.*

$$\begin{aligned} \mathcal{E}_{-n} &= E_n + \frac{1}{2} i\Gamma_n, \quad \Gamma_n > 0\,, \\ \Psi_{-n}(\mathbf{r}, t) &= \psi^*_n(\mathbf{r}) \exp(-iE_n t) \exp(\Gamma_n/2t)\,. \end{aligned} \tag{4}$$

These states grow in time and are often referred as antiresonant states (antiresonances). In the above and further in this paper, Rydberg units, *i.e.* $\hbar = 1$ and $m = 1/2$, where m is the particle mass (for example, the effective mass of an electron in a semiconductor) are used.

As mentioned, the states given by Eqs. (3) are indeed resonant states, provided that $\psi_n(\mathbf{r})$ satisfy the outgoing boundary conditions. To impose these conditions, it is convenient to characterize the resonant states by the complex eigenwavenumber $k_n = \alpha_n + i\,\beta_n$, where $\alpha_n = \mathrm{Re}(k_n)$ and $\beta_n = \mathrm{Im}(k_n)$, related to the complex energy $\mathcal{E}_n$ as

$$\mathcal{E}_n = k_n^2 = \alpha_n^2 - \beta_n^2 + 2i\alpha_n\beta_n. \tag{5}$$

The outgoing boundary conditions select from a pool of functions $\psi_n(\mathbf{r})$, satisfying Eq. (1), only those obeying

$$\psi_n(\mathbf{r}) \sim e^{i\alpha_n r}\, e^{-\beta_n r},\ \alpha_n > 0, \quad r \to \infty. \tag{6}$$

The resonant states $\psi_n(\mathbf{r})$ have then $\beta_n < 0$ as $\Gamma_n > 0$ in Eq. (2), *i.e.* their eigenwavenumbers k_n are located in the fourth quadrant of the complex wave number plane. The states are not orthogonal and not normalizable in the usual way, see Refs. [7–9].

The antiresonant states $\psi_{-n}(\mathbf{r}) = \psi^*_n(\mathbf{r})$ satisfy the asymptotic condition

$$\psi_{-n}(\mathbf{r}) \sim e^{-i\alpha_n r}\, e^{-\beta_n r}, \quad r \to \infty. \tag{7}$$

Their eigenwavenumbers $k_{-n} = \alpha_{-n} + i\beta_{-n} = -\alpha_n + i\beta_n$ are located in the third quadrant of the complex wave number plane.

A special case $\alpha_n = 0$ corresponds to real negative energies $\mathcal{E}_n = E_n = -\beta_n^2 < 0$. It includes either the bound states with $\beta_n > 0$ and coordinate wave functions $\psi_n(\mathbf{r})$ vanishing far from the potential, or antibound states with $\beta_n < 0$ and purely growing functions $\psi_n(\mathbf{r})$ outside of the potential.

As one can see, we defined the resonant/antiresonant states as explicit solutions of the Schrödinger equation with complex eigenvalues and eigenfunctions subject to the boundary conditions given by Eqs. (6, 7). This is an approach illustrated in Refs. [8–11]. Another way to introduce these states is to associate them with the poles of the outgoing Green's function, see Refs. [8, 9], or with the poles of the scattering matrix S, see Refs. [12, 13].

* gregory.morozov@uws.ac.uk

The purpose of this paper is to understand how the resonant/antiresonant states evolve, develop and possibly transform into bound states of a quantum mechanical system. This is an interesting and useful exercise, especially in the context of a newly-adopted resonant-state expansion method, see Refs. [14–17]. The complex wave number plane provides one option of a natural setting in which to pursue this, see Refs. [11–13, 18] for the 1D quantum problem and Refs. [19, 20] for the 2D quantum problem. In this paper, however, using a square well/barrier as an example, we present an alternative complex plane, which we call the *potentiodynamic* wave number coordinate system. In this plane we can learn more about the behavior of the full spectrum of eigenstates of Eq. (1), especially in the limit of large potentials. As a result, the square well/barrier potential system will serve as a proof of concept for potentiodynamic coordinates before applying the technique in a more complicated setting where special functions often feature, obfuscating the details.

II. RESONANT STATES OF SQUARE WELL POTENTIAL

The square well potential of width $2a$ is defined as

$$V(z) = \begin{cases} 0, & |z| > a, \\ -V_0, & |z| < a, \end{cases} \tag{8}$$

where $V_0 > 0$. Eq. (1) takes the form

$$\begin{aligned} &\psi''(z) + k^2\psi(z) = 0, \quad k = \sqrt{\mathcal{E}}, \qquad\quad |z| > a, \\ &\psi''(z) + \kappa^2\psi(z) = 0, \quad \kappa = \sqrt{k^2 + V_0}, \quad |z| < a, \end{aligned} \tag{9}$$

where all three parameters involved, $\mathcal{E}$, k, and κ, have in general complex values. A general solution of Eq. (9) can be represented as

$$\begin{aligned} \psi(z) &= A\exp(ikz) + B\exp(-ikz), \; z < -a, \\ \psi(z) &= F\cos(\kappa z) + G\sin(\kappa z), \quad -a < z < a, \\ \psi(z) &= C\exp(ikz) + D\exp(-ikz), \; z > a. \end{aligned} \tag{10}$$

The boundary conditions given by Eqs. (6, 7), where for the 1D case, r should be replaced by z, require $A = D = 0$. Further, the continuity requirements for $\psi(z)$ and $\psi'(z)$ at the points $z = -a$ and $z = a$ lead to the complex transcendental equation

$$2k\kappa\cos(2\kappa a) - i(k^2 + \kappa^2)\sin(2\kappa a) = 0, \tag{11}$$

whose solutions are the complex eigenwavenumbers $k_{\pm n}$ of the corresponding resonant/antiresonant states. The above transcendental equation can also be written in the form

$$\tan(2\kappa a) + i\frac{2(ka)(\kappa a)}{(ka)^2 + (\kappa a)^2} = 0, \tag{12}$$

or

$$\left[\tan(\kappa a) + i\frac{ka}{\kappa a}\right]\left[\tan(\kappa a) + i\frac{\kappa a}{ka}\right] = 0. \tag{13}$$

We should note that since for a square well potential $V(z) = V(-z)$, a general solution of Eq. (9) can be represented as a superposition of a symmetric solution $\psi_1(z) = \psi_1(-z)$ and an antisymmetric one $\psi_2(z) = -\psi_2(-z)$. It then happens that solutions corresponding to resonant/antiresonant states, see Eqs. (10) with $A = D = 0$, are either symmetric or antisymmetric. In particular, the symmetric resonant/antiresonant state $\psi^s_{\pm n}$ is

$$\psi^s_{\pm n}(z) = \begin{cases} \exp(-ik_{\pm n}z), & z < -a, \\ F\cos(\kappa_{\pm n}z), & -a < z < a, \\ \exp(ik_{\pm n}z), & z > a, \end{cases} \tag{14}$$

with the corresponding eigenwavenumber $k_{\pm n}$ determined by the first factor in Eq. (13). The antisymmetric resonant/antiresonant state $\psi^a_{\pm n}$ is

$$\psi^a_{\pm n}(z) = \begin{cases} \exp(-ik_{\pm n}z), & z < -a, \\ G\sin(\kappa_{\pm n}z), & -a < z < a, \\ -\exp(ik_{\pm n}z), & z > a, \end{cases} \tag{15}$$

with the corresponding eigenwavenumber $k_{\pm n}$ determined by the second factor in Eq. (13).

At this point we should reiterate that for the bound states the wavenumber $k = \alpha + i\beta$ is restricted to the subset of positive imaginary values. As the energies of the bound states satisfy the condition $\mathcal{E} = E = -\beta^2 > -V_0$, the parameter $\kappa = \sqrt{k^2 + V_0}$ takes positive real values. Then, Eq. (13) is reduced to the two well-known conditions, $\kappa a \tan\kappa a = \beta a$ and $\kappa a \cot\kappa a = -\beta a$, where $\kappa^2 + \beta^2 = V_0$, for the even and odd bound states respectively, see, for example, Refs. [21, 22].

As mentioned in the introduction, another way to find resonant/antiresonant states is to build the scattering S-matrix and identify its poles. In general, the S-matrix of an arbitrary 1D potential with the compact support (the potential is zero outside of a finite interval) is given by

$$S = \begin{bmatrix} r_L & t \\ t & r_R \end{bmatrix}, \tag{16}$$

where r_L is the reflection coefficient for left incidence, r_R is the reflection coefficient for the right incidence, and $t_L = t_R \equiv t$ is the transmission coefficient.

To find the left scattering solution for the square well potential, *i.e.* r_L and $t_L = t$, one should put $A = 1$, $B = r_L$, $C = t_L$, and $D = 0$ in the general solution given by Eq. (10), and apply continuity requirements at $z = \pm a$. To find the right scattering solution, *i.e.* r_R and $t_R = t$, one should put $D = 1$, $C = t_R$, $B = r_R$, and $A = 0$ in Eq. (10), and apply continuity requirements at

$z = \pm a$ again. This will lead to

$$r_L = r_R = \frac{-i(k^2 - \kappa^2)\sin(2\kappa a)}{2k\kappa\cos(2\kappa a) - i(k^2 + \kappa^2)\sin(2\kappa a)},$$
$$t = \frac{2k\kappa}{2k\kappa\cos(2\kappa a) - i(k^2 + \kappa^2)\sin(2\kappa a)}. \tag{17}$$

We should note that scattering solutions do not have any particular symmetry. As expected, the poles of the S-matrix are given by Eqs. (11) - (13).

III. FLOWS

In this section, first, we numerically solve Eq. (11) to find the locations of the resonances/antiresonances $k_{\pm n}$ in the complex wave number (ka) plane and then follow their trajectories in response to varying the depth of the well. The trajectories traced out in this procedure are known as *flows*, and a plot of all flows we call the *flow portrait*. As mentioned in the introduction, in this paper we also intend to reveal new features of flow behavior using an alternative (*potentiodynamic*) complex plane. For a square well potential we define *potentiodynamic* coordinates as $\mathrm{Re}(\kappa a)$, $\mathrm{Im}(\kappa a)$, where

$$\kappa a = \sqrt{k^2 + V_0}\, a\,. \tag{18}$$

Thus, we also follow the trajectories of the solutions of Eq. (11) in the complex potentiodynamic coordinates (κa) in response to varying the depth of the well. What emerges is a deep insight into the connection between the different types of states, and their interconversion.

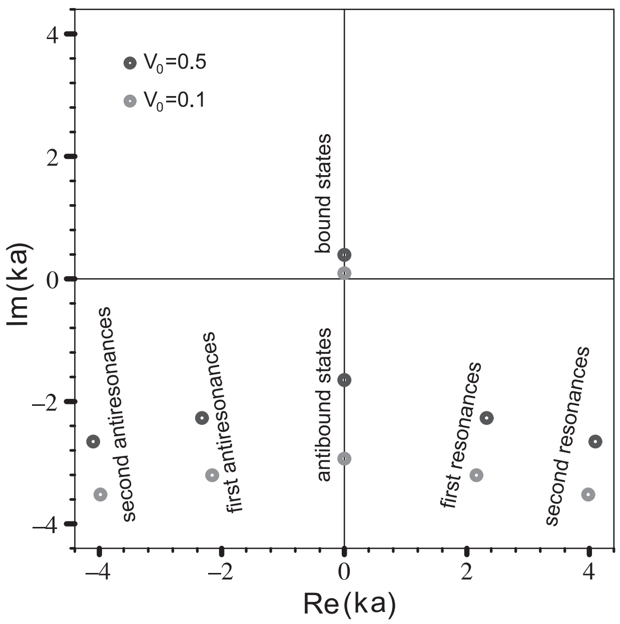

FIG. 1. Complex eigenwavenumbers of the eigenstates of the square well potential of width $2a$ for two fixed values of potential depth V_0.

We begin our analysis by finding solutions of Eq. (11) for two relatively shallow wells of $V_0 = 0.1$ and $V_0 = 0.5$. The results are shown in Fig. 1. All four possible kinds of eigenstates mentioned earlier (bound states, antibound states, resonances, and antiresonances) are encountered. We should note that the square root function in Eq. (18) is a double-valued one. To choose the proper values (the proper Riemann sheet) for the potentiodynamic coordinates κa, we will use the condition

$$\kappa a \to ka\,, \quad V_0 \to 0. \tag{19}$$

In Fig. 2 we analyze the flows which originate from bound and antibound states of infinitesimally shallow wells. It is known that there always exists a bound state (the ground bound state) for an arbitrarily shallow square well potential; as the well is deepened the ground bound state moves up, see the right flow on the upper panel of Fig. 2. The limit values of eigenwavenumbers k_g of ground bound states are then

$$k_g\, a \to 0,\, V_0 \to 0, \quad k_g\, a \to i\infty,\, V_0 \to \infty. \tag{20}$$

On the negative imaginary axis there are antibound states; as the well is deepened the antibound state also moves up and eventually becomes the first excited bound state, see the left flow on the upper panel of Fig. 2. The limit values of eigenwavenumbers k_a of (originally) antibound states are then

$$k_a\, a \to -i\infty,\, V_0 \to 0, \quad k_a\, a \to i\infty,\, V_0 \to \infty. \tag{21}$$

The corresponding flows in κa coordinates are shown on the lower panel of Fig. 2. The flow of ground bound states is on the positive real axis within the interval given by $0 < \kappa_g\, a < \pi/2$, and the limit values are

$$\kappa_g\, a \to 0,\, V_0 \to 0, \quad \kappa_g\, a \to \pi/2,\, V_0 \to \infty. \tag{22}$$

The flow of antibound states in κa coordinates goes initially along the negative imaginary axis, but turns onto the positive real axis at the origin $\kappa_a a = 0$ (where $k_a a = -i$), and later at the point $\kappa_a a = \pi/2$ (where $k_a a = 0$) becomes the first excited bound state. The corresponding limit values are then

$$\kappa_a\, a \to -i\infty,\, V_0 \to 0, \quad \kappa_a\, a \to \pi,\, V_0 \to \infty. \tag{23}$$

In Fig. 3 we illustrate the behavior of the flows which originate from resonant/antiresonant states of infinitesimally shallow wells. The starting points of the flows in the wave number plane, *i.e.* the limit values of their eigenwavenumbers k_m and k_{-m} in the opening limit, are

$$k_{\pm m} a \to \pm m\pi/2 - i\infty,\, V_0 \to 0,\, m = 1, 2, \ldots\,. \tag{24}$$

The corresponding resonance/antiresonance pairs coalesce at the attractor $ka = -i$, see the upper panel of Fig. 3. This leads to the creation of two antibound states: one of which moves up along the imaginary axis, becomes bound, and goes further up towards $i\infty$; the

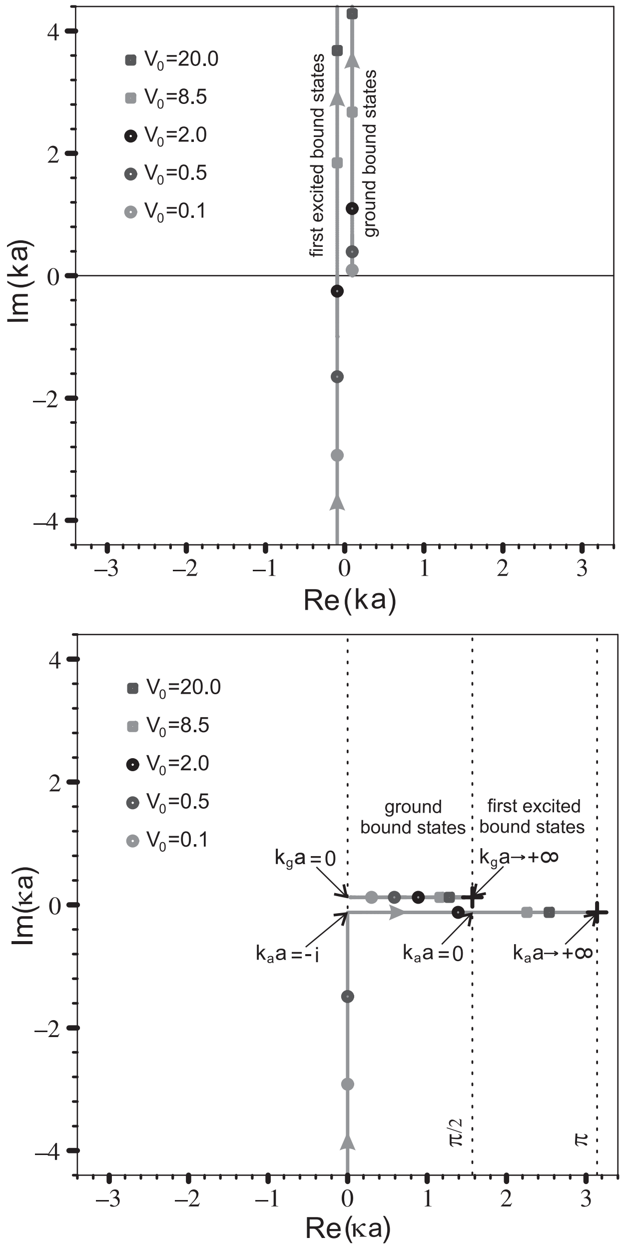

FIG. 2. Flows of the ground bound state and first antibound state (which becomes the first excited bound state) as V_0 is deepened beginning from effectively zero depth. In ka coordinates [upper panel], the flow of the ground bound state starts at the origin and goes to $(0, +i\infty)$. In κa coordinates [lower panel], the corresponding flow starts at the origin and goes to $(\pi/2, 0)$. In ka coordinates [upper panel], the flow of the first antibound state (leading to the first excited bound state) starts at $(0, -i\infty)$ and goes to $(0, +i\infty)$. In κa coordinates [lower panel], the corresponding flow starts at $(0, -i\infty)$, turns onto the positive real axis, converts into the first excited bound state at $(\pi/2, 0)$, and goes along the positive real axis to $(\pi, 0)$. The limit points of the flows in κa coordinates for $V_0 \to \infty$ are shown as crosses and occur at at $(\pi/2, 0)$ and $(\pi, 0)$. Note that the flows are offset from the relevant axes to reveal the presence of two flows where they coincide.

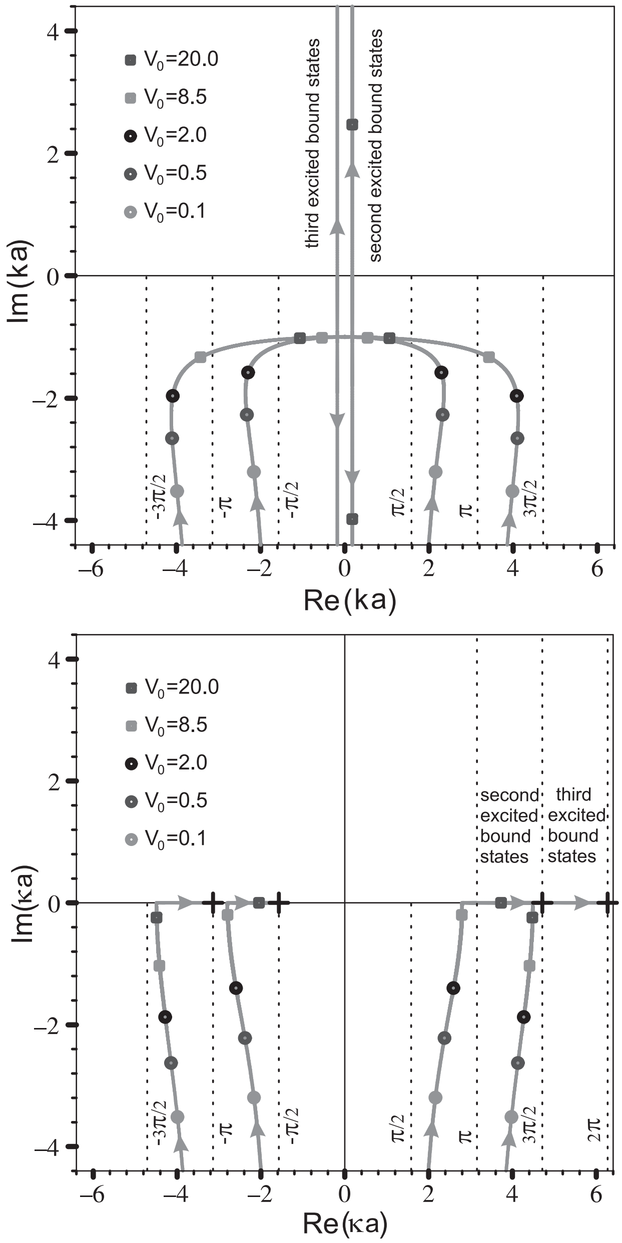

FIG. 3. Coalescence of the first and second resonance and antiresonance flows occurs at the attractor $-i$ in the ka plane [upper panel]. The limit points of the first and second resonance flows in κa coordinates [lower panel] for $V_0 \to \infty$ are shown as crosses and occur at $(3\pi/2, 0)$ and $(2\pi, 0)$. The limit points of the first and second antiresonance flows in κa coordinates for $V_0 \to \infty$ are also shown as crosses and occur at $(-\pi/2, 0)$ and $(-\pi, 0)$ respectively. Note that the flows in upper panel are offset from the vertical axes to reveal the presence of two flows there.

other one goes down along the imaginary axis towards $-i\infty$. Therefore, none of these flows remain bounded in the wave number plane when $V_0 \to \infty$.

The starting points of the resonance/antiresonance flows in κa coordinates in the opening limit, see lower panel in Fig. 3, are the same as in ka coordinates, see

Eq. (19), *i.e.*

$$\kappa_{\pm m} a \to \pm m\pi/2 - i\infty,\ V_0 \to 0,\ m = 1, 2, \ldots. \qquad (25)$$

The flows reach the real axis at the points defined by the real-valued solutions of equation

$$[\tan(\kappa a) + 1/\kappa a]\,[\tan(\kappa a) - \kappa a] = 0, \qquad (26)$$

which follow from Eq. (13), where we took into account that $ka = -i$. Then, the antibound state generated from the m-th antiresonance flow moves to the right along the real axis towards $-m\pi/2$, *i.e.*

$$\kappa_{-m} a \to -m\frac{\pi}{2},\ V_0 \to \infty, \qquad (27)$$

while the antibound state generated from the m-th resonance becomes bound upon crossing the point $(m+1)\,\pi/2$ and goes further to the right towards $(m+2)\,\pi/2$, *i.e.*

$$\kappa_m a \to (m+2)\,\frac{\pi}{2},\ V_0 \to \infty. \qquad (28)$$

In particular, the first resonance flow reaches the real axis at the point $\kappa a \cong 2.798$. Then, a newly created antibound state moves to the right, becomes a bound state upon crossing the point $\kappa a = \pi$, and goes towards $\kappa a = 3\pi/2$ when $V_0 \to \infty$. The second resonance flow reaches the real axis at the point $\kappa a \cong 4.493$. Then, a newly created antibound state moves to the right, becomes a bound state upon crossing the point $\kappa a = 3\pi/2$, and goes towards $\kappa a = 2\pi$ when $V_0 \to \infty$.

Overall, transformation to the potentiodynamic plane results in a bounding of all the flows when $V_0 \to \infty$, with the limiting values being integer multiples of $\pi/2$ on the real axis. The fact that the flows are bounded for arbitrarily deep wells in the potentiodynamic plane makes it a useful tool not only for determining the asymptotic behavior of the states, but also for comparing the finite well with the infinite analogue. Such a comparison is usually done, see, for example, Ref. [22], by making an upward shift of the zero energy level by V_0, *i.e.* transforming the potential given by Eq. (8) into $V(z) = V_0$ for $|z| > a$ and $V(z) = 0$ for $|z| < a$, and resolving the corresponding transcendental equations with $V_0 \to \infty$ for real-valued energies $\mathcal{E}$. Here, using that for $V_0 \to \infty$, the corresponding bound state κ eigenvalues are given by $\kappa_g a \to \pi/2$, $\kappa_a a \to \pi$, and $\kappa_m a \to (m+2)\,\pi/2$, see Eqs. (22, 23, 28), we immediately obtain the results for the bound state energies of the infinite square well of width $2a$ in the form

$$\begin{aligned} \mathcal{E}_n &= -V_0 + \frac{n^2\pi^2}{(2a)^2},\ n = 1, 2 \ldots \text{ (Rydberg units)}, \\ \mathcal{E}_n &= -\frac{\hbar^2}{2m}V_0 + \frac{n^2\pi^2\hbar^2}{2m(2a)^2} \qquad \text{(normal units)}. \end{aligned} \qquad (29)$$

IV. SQUARE BARRIER

To complete considerations of 1D square potentials, we also treat the case of a 1D square barrier, which is actually much simpler to interpret. The square barrier potential of width $2a$ is defined as

$$V(z) = \begin{cases} 0, & |z| > a, \\ V_0, & |z| < a,\ V_0 > 0. \end{cases} \qquad (30)$$

To find and analyze its resonances one needs to follow all steps in Section II. In particular, Eqs. (9) - (17) are also applicable to the barrier case, if the potentiodynamic

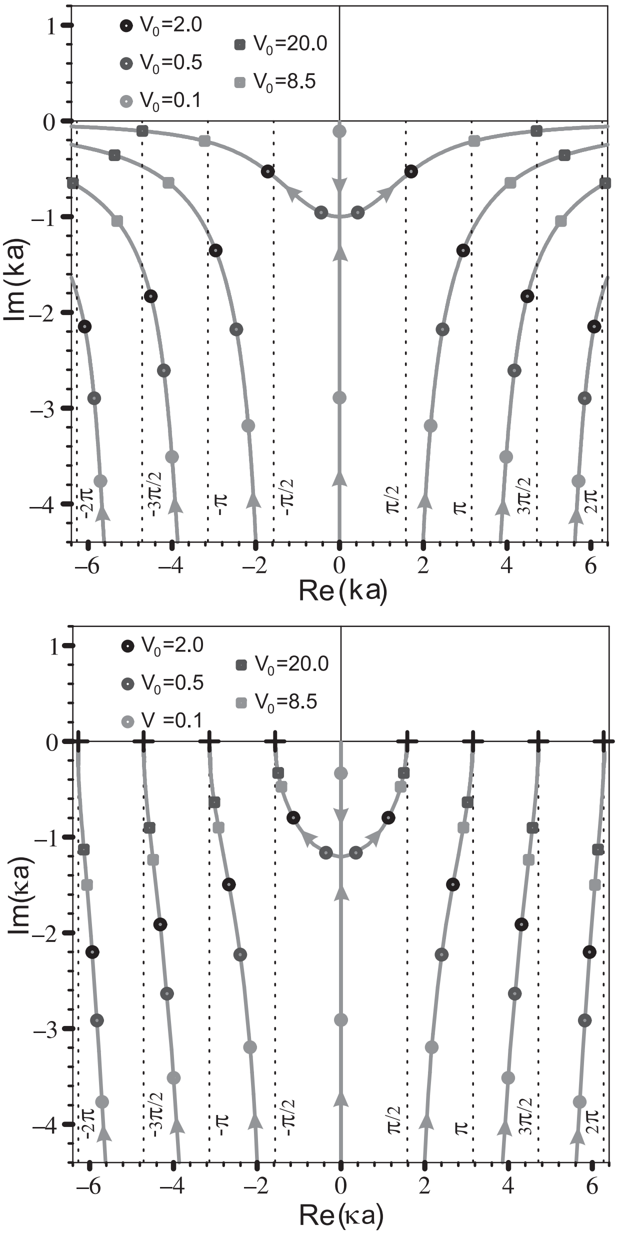

FIG. 4. Flow portraits of the resonances of the square barrier in the ka (upper panel) and in the κa (lower panel) planes. The limit points of the resonance and antiresonance flows in κa coordinates for $V_0 \to \infty$ are shown as crosses and occur at $(m\pi/2, 0)$ and $(-m\pi/2, 0)$ respectively.

parameter κ is redefined as

$$\kappa = \sqrt{k^2 - V_0}, \quad V_0 > 0. \tag{31}$$

The overall flow portrait in ka coordinates is shown in the upper panel of Fig. 4. For the very low barrier there are two antibound states: one is close to the origin (in particular, for this state $ka \to 0$, if $V_0 \to 0$), and the other is located deep on the negative imaginary axis (in particular, for this state $ka \to -i\infty$, if $V_0 \to 0$). As the potential V_0 grows these two antibound states move towards each other, then annihilate at the $ka = -i$ coalescence point, generating the first, counting from the real axis, flows of resonant, k_1, and antiresonant, k_{-1}, states. The flows which originate from resonant/antiresonant states of infinitesimally low barriers behave as follows. Their starting points in the wave number plane, *i.e.* the limit values of their eigenwavenumbers k_m and k_{-m} in the opening limit, are given by

$$k_{\pm m}a \to \pm(m-1)\frac{\pi}{2} - i\infty, \; V_0 \to 0, \; m = 2, 3, \ldots. \tag{32}$$

As the barrier grows, the resonant states move up and to the right, while the antiresonant states move up and to the left, never coupling with one another, and with asymptotic values given by

$$k_{\pm m}a \to \pm\infty - 0\,i, \; V_0 \to \infty, \; m = 1, 2, 3, \ldots. \tag{33}$$

As expected no resonances exist for the impenetrable barrier.

The overall flow portrait in κa coordinates is shown in the lower panel of Fig. 4. In these coordinates, two antibound states appearing for lower barriers also move towards each other but annihilate at $\kappa a \cong -1.200i$, which is one of the two complex-valued (conjugate) solutions of Eq. (26). The first generated flows of resonant/antiresonant states as well as the flows which originate from resonant/antiresonant states of infinitesimally low barriers remain bounded and behave asymptotically as

$$\kappa_{\pm m}a \to \pm m\frac{\pi}{2}, \; V_0 \to \infty, \; m = 1, 2, 3, \ldots. \tag{34}$$

V. CONCLUSIONS

In this paper we studied the flows of resonances (antiresonances) for the square well potential. In particular, beginning with a very shallow well, it was illustrated how these states appear, develop, and possibly transform into bound states in response to increasing the depth of the well. Along with the complex wave number plane, the results were illustrated in a newly introduced potentiodynamic complex plane. We have shown that the potentiodynamic plane is a useful new addition to the tools that already exist for probing the dynamical behavior of resonant states. It provides an illuminating way to keep track of the asymptotics of the flows by ensuring that their trajectories remain bounded, a feature which follows from the incorporation of the potential as an intrinsic part of the coordinate system. It seems to us that this coordinate system will be useful for comparison of analogous finite and infinite potential systems, and in particular, that it can be used alongside the standard wave number plane to get a clearer picture of what happens to the unbounded flows in the standard coordinate plane.

[1] A. B. Matsko, *Practical Applications of Microresonators in Optics and Photonics* (CRC Press, 2009).
[2] N. Jokerst, M. Royal, S. Palit, L. Luan, S. Dhar, and T. Tyler, J. Biophotonics **2**, 212 (2009).
[3] J. Zhu, S. K. Ozdemir, Y.-F. Xiao, L. Li, L. He, D.-R. Chen, and L. Yang, Nat. Photonics **4**, 46 (2010).
[4] M. F. Limonov, M. V. Rybin, A. N. Poddubny, and Y. S. Kivshar, Nat. Photonics **11**, 543 (2017).
[5] G. Gamow, Z. Phys. **51**, 204 (1928).
[6] A. F. J. Siegert, Phys. Rev. **56**, 750 (1939).
[7] R. M. More and E. Gerjuoy, Phys. Rev. A **7**, 1288 (1973).
[8] R. Madrid and M. Gadella, Am. J. Phys. **70**, 626 (2002).
[9] G. Garcia-Calderon and J. Villavicencio, Phys. Rev. A **99**, 022108 (2019).
[10] Z. Ahmed, S. Pavaskar, and L. Prakash, Eur. J. Phys. **36**, 048001 (2015).
[11] R. Zavin and N. Moiseyev, J. Phys. A: Math. Gen. **37**, 4619 (2004).
[12] H. M. Nussenzveig, Nucl. Phys. **11**, 499 (1959).
[13] B. Belchev, S. G. Neale, and M. A. Walton, Can. J. Phys. **89**, 1127 (2011).
[14] E. A. Muljarov, W. Langbein, and R. Zimmermann, EPL **92**, 50010 (2010).
[15] M. B. Doost, W. Langbein, and E. A. Muljarov, Phys. Rev. A **87**, 043827 (2013).
[16] M. B. Doost, W. Langbein, and E. A. Muljarov, Phys. Rev. A **90**, 013834 (2014).
[17] A. Tanimu and E. A. Muljarov, Phys. Rev. A **98**, 22127 (2018).
[18] D. W. L. Sprung, H. Wu, and J. Martorell, Am. J. Phys. **64**, 136 (1996).
[19] R. P. Meeten, G. S. Docherty-Walthew, and G. V. Morozov, Phys. Rev. A **99**, 042126 (2019).
[20] R. P. Meeten and G. V. Morozov, Physica E: Low-dimensional Systems and Nanostructures **118**, 113917 (2020).
[21] D. J. Griffiths, *Introduction to Quantum Mechanics, Second Edition* (Cambridge University Press, 2016).
[22] B. H. Bransden and C. J. Joachain, *Quantum Mechanics, Second Edition* (Prentice Hall, 2000).